Robust Feature for Transcranial Sonography Image Classification Using Rotation-Invariant Gabor Filter

Arkan Al-Zubaidi[1], Lei Chen[1,3], Johann Hagenah[2], Alfred Mertins[1]

[1]Institute for Signal Processing, University of Luebeck,Germany
[2]Department of Neurology, University Hospital Schleswig-Holstein, Germany
[3]Graduate School, University of Luebeck, Germany
chen@isip.uni-luebeck.de

Abstract. Transcranial sonography is a new tool for the diagnosis of Parkinson's disease according to a distinct hyperechogenic pattern in the substantia nigra region. In order to reduce the influence of the image properties from different settings of ultrasound machine, we propose a robust feature extraction method using rotation-invariant Gabor filter bank. Except the general Gabor features, such as mean and standard deviation, we suggest to use the entropy of the filtered images for the TCS images classification. The performance of the Gabor features is evaluated by a feature selection method with the objective function of support vector machine classifier. The results show that the rotation-invariant Gabor filter is better than the conventional one, and the entropy is invariant to the intensity and the contrast changes.

1 Introduction

Transcranial sonography (TCS) was first used in 1995 to distinguish between a group of Parkinson's disease (PD) patients and healthy controls by Becker et al. [1]. For the healthy controls, the hyperechogenicity of the substantia nigra (SN) was significantly decreased compared to PD patients. It is possible to determine the structure of the idiopathic from of Parkinsonism at an early state by means of TCS technique [2]. However, the structural abnormalities were not detected on CT and MRI scans [3]. Three feature analysis algorithms were implemented based on the ipsilateral mesencephalon wing, which is close to the ultrasound probe as shown in Fig. 1. First, the moment of inertia and Hu1-moment were calculated based on manually segmented half of mesencephalon (HoM) for separating control subjects from Parkin mutation carriers [4]. Then, a hybrid feature extraction method, which includes statistical, geometrical and texture features for the early PD risk assessment, was proposed [5], It showed a good performance of texture features, especially Gabor features. Third, a texture analysis method that applied a bank of Gabor filters and gray-level co-occurrence matrices (GLCM) was used on TCS images [6]. In this paper, we used three datasets that were acquired by different examiners with in different

H.-P. Meinzer et al. (Hrsg.), *Bildverarbeitung für die Medizin 2013*, Informatik aktuell,
DOI: 10.1007/978-3-642-36480-8_48,

periods. These datasets include the TCS images from the healthy controls (HC) and PD patients. The properties of the TCS images, such as the contrast and brightness, are effected by different setting of the US machine used by different examiners. Furthermore, the challenge of the classification of the TCS images using Gabor filters is that orientations and shapes of the HoM are different from one PD patient to another.

2 Methods

Our goal is to develop Gabor features that are invariant to the direction of HoM, the brightness and the contrast changes from the different settings. Therefore, we propose a texture analysis method that applies a rotation-invariant Gabor filter bank on the HoM area and computes the histogram feature from the filtered images for the TCS image classification.

2.1 Conventional gabor filter bank

The performance of conventional Gabor filters becomes poor if texture can occur with arbitrary orientations [7, 8]. Let I(x, y) be an image, its discrete Gabor wavelet transform is defined by a convolution

$$\mathrm{G_{mn}(x,y)} = \sum_{\xi} \sum_{\eta} \mathrm{I(x-\xi, y-\eta) g^{*}_{mn}}(\xi, \eta) \tag{1}$$

where parameters m and n specify the scales and orientations, respectively, and * indicates the complex conjugate of g_{mn} [9]. The 2D Gabor function $g(\xi, \eta)$ is

$$\mathrm{g}(\xi, \eta) = \frac{1}{2\pi\sigma_{\xi}\sigma_{\eta}} \exp[-\frac{1}{2}(\frac{\xi^2}{\sigma_{\xi}^2} + \frac{\eta^2}{\sigma_{\eta}^2})] \cdot \exp[2\pi \mathrm{j W} \xi] \tag{2}$$

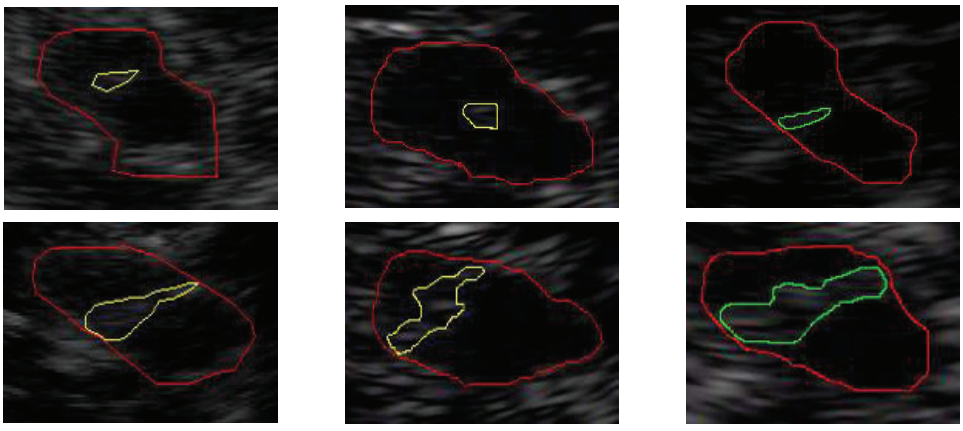

Fig. 1. Manually segmented TCS images with Philips SONOS 5500. The first and second row are from healthy control subjects and PD patients, respectively. The red marker indicates the upper HoM. Yellow/green markers show the SN area.

where W is called the modulation frequency, the other parameters are chosen as in [6]. It is assumed that the SN region in the ROI (HoM) has homogeneous texture, therefore the mean μ_{mn} and the standard deviation σ_{mn} of the coefficients' magnitudes are used to represent the texture features in the conventional Gabor feature vector f_c as in [6]. The filter mask size is 61×61, five scales and six orientations have been used in the experiments.

2.2 Rotation-invariant gabor filter design

Han et al. [7] proposed the summation of all the Gabor filter responses under different orientations, but along the same scale, could yield a rotation-invariant Gabor filter

$$\mathrm{g}_{\mathrm{m}}^{(\mathrm{R})}(\xi,\eta) = \sum_{\mathrm{n}=0}^{\mathrm{K}-1} \mathrm{g}_{\mathrm{m,n}}(\xi,\eta), \mathrm{m} = 0, 1, ..., \mathrm{S}-1 \tag{3}$$

Zhang et al. [8] suggested to sort the Gabor features by the total energy of the filtered images over the orientation with the same scale. The orientation of filtered image with the highest total energy is defined as the dominant direction. An example texture image and the energy map are shown in Fig. 2 (a) and (b), respectively. The rotated image (90^o of the first image) and the corresponding energy map are shown in Fig. 2 (c) and (d), respectively. Fig. 2 (b) shows that image (a) has a dominant direction at orientation 5 (150^o), while for image (c), the dominant direction has moved to orientation 2 (30^o). Using the same concept, the filtered image G_{ij} with the dominant direction j is moved to be at the first position at scale i, and the other filtered images are circularly shifted accordingly. As a result, the feature elements μ_{ij}, σ_{ij} in conventional Gabor feature vector f_c are shifted as in the rotation-invariant Gabor feature vector f_r. For example, if f_c is (A,B,C,D,E,F) and (C) is at the dominant direction, then f_r is (C,D,E,F,A,B).

2.3 Robust feature extraction

In gerenal, the conventional Gabor features, the mean and the standard deviation are calculated from the intensity values of the filtered image directly. In this section, we compute the entropy from the histogram of the filtered image. Shannon entropy can be used to measure the randomness of the image histogram.

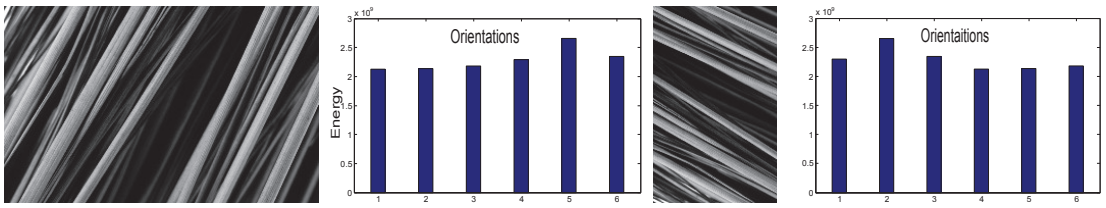

(a) Grass image (b) Energy map (c) 90^o (d) Energy map

Fig. 2. Texture image and the energy map of the filtered images at each orientation.

In other words, the entropy measures the uniformity of the filtered image. In Fig. 3, the TCS images were normalized to the range [0,255], then the method of Zhang et al. was used to extract the features from HoM region. The result shows that the mean and standard deviation features from ROI are changed but the entropy feature of the histogram is more stable. Actually, the symbol alphabet of filtered image is in general not finite. Therefore, a proper measurement of entropy is differential entropy [10]. The entropy of the histogram image is given

$$H(X) = -\sum_{x \in S} \mathrm{hist}_{\mathrm{norm}}(x) \log_2(\mathrm{hist}_{\mathrm{norm}}(x)) \tag{4}$$

where S is the support set of the random variable x and $\mathrm{hist}_{\mathrm{norm}}(\mathrm{x})$ is the histogram properly normalized to fit a probability density function. The summation of the probability density function $\mathrm{hist}_{\mathrm{norm}}(\mathrm{x})$ is one. In our case, the complete feature vector F of the rotation-invariant Gabor filter has 90 dimensions: $F(1, ..., 60)$ are 60 Gabor features $\mu_{\mathrm{ij}}, \sigma_{\mathrm{ij}}$ in feature vector $f_r(1, 2, ..., 60)$; $F(61, ..., 90)$ are 30 features of entropy $f_{\mathrm{re}}(1, 2, ..., 30)$.

3 Method of evaluation

The normalization process is used to simulate different user settings. Brightness and contrast changes were applied to the TCS images. In this paper, three normalization methods are tested on the TCS images. The first normalization is zero mean and unit variance ($\frac{X-\mu}{\sigma}$). Second, all TCS images are rescaled to full gray level range [0,255]. Third, we applied the contrast-limited adaptive histogram equalization (CLAHE) [11] to match the histogram of ROI with a desired shape. The exponential and Rayleigh distributions were used in this experiment. Furthermore, the Gabor features were evaluated by the sequential forward floating selection (SFFS) method. The accuracy of the SVM classifier was used as a criterion function of SFFS. The sequential minimal optimization (SMO) method

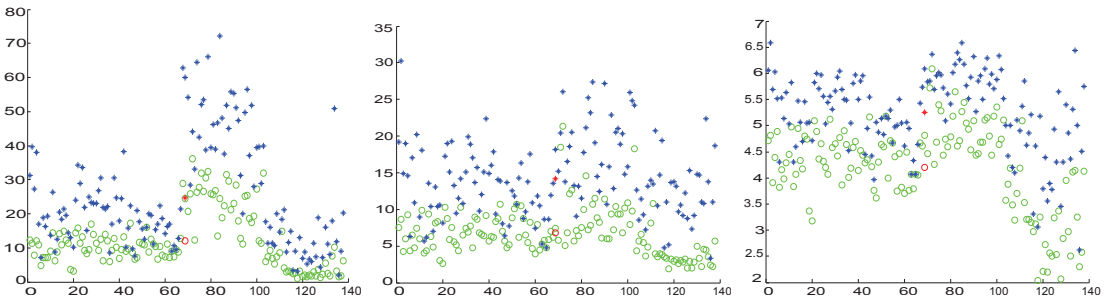

(a) μ Feature (b) σ Feature (c) Entropy Feature

Fig. 3. Green circles: Features of the original images. Blue stars: Features of the rescaled images ([0,255]). Red points: Mean value of the features. Under the rescaling the mean value of the μ and the σ features are shifted from 11 to 26, and shifted from 7 to 14, respectively. But the entropy features are more stable than μ, and the σ features, the corresponding mean value only shifted from 4.1 to 5.2.

Table 1. Performance of Gabor filter banks on the public dataset [12].

SVMs cross-validation	Conventional Gabor	Zhang et al. [8]	Han et al. [7]
Accuracy	72%	76%	72%
Confusion matrix	$\begin{pmatrix} 39 & 1 \\ 21 & 19 \end{pmatrix}$	$\begin{pmatrix} 40 & 0 \\ 19 & 21 \end{pmatrix}$	$\begin{pmatrix} 38 & 2 \\ 20 & 20 \end{pmatrix}$

and the linear kernel were specified to find the separating hyperplane. The cross validation was set with the leave-one-out method.

We compared the rotation-invariant Gabor filter algorithms according to the UIUC database [12]. We selected T01(bark1) and T15(brick2) from that database. These are two rotated texture sets, each one containing 40 samples. The results in Tab. 1 show that the method of Zhang et al. [8] works better than the method of Han et al. [7] and the conventional Gabor filter method.

4 Experimental results

The classification results were based on three datasets of TCS images, which were obtained using Philips SONOS 5500 by different examiners. Dataset 1 includes 36 TCS images from 21 healthy subjects and 42 TCS images from 23 PD patients. Dataset 2 includes 8 control TCS images from 4 healthy subjects and 15 PD TCS images from 10 patients. The last dataset consisted of 27 control TCS images from 14 healthy subjects and 10 PD TCS images from 5 patients. Totally, this dataset includes 67 PD images from 38 PD patients and 71 control images from 39 healthy subjects. The Gabor filter bank was applied to the ROI of TCS images. Then, the rotation-invariant Gabor features were extracted and shifted by the dominant direction. The feature extraction from the manual segmentation of HoM, which was marked by the physicians as shown in Fig. 1. The feature analysis results in Tab. 2 show that the entropy features $F(61, 77)$ are more stable than the mean and the standard deviation features $F(1, 5, 7)$. The feature subset $F(66, 3)$ obtained by $SFFS$ gave the highest classification rate of 81.88% ($F(66)$ is the entropy feature $f_{\mathrm{re}}(6)$ and $F(3)$ is the mean feature $f_r(3)$). The results in the right two columns of Tab. 2 show the performance of the feature sets with different methods of image normalization, and the confusion matrices for the feature set $F(66, 3)$. At last, based on this dataset, the features of the conventional Gabor filter in [6] achieved 69.56% classification rate. In this paper, the accuracy reached 81.88% which is better than the method of Chen et al. [6], and the histogram feature is more stable.

5 Conclusions

This paper has concentrated on the texture analysis of the HoM and even the SN area by using rotation-invariant Gabor filters and selecting good combinations of features for PD detection. The accuracy of the classification results shows

Table 2. Classification results of rotation-invariant Gabor filter banks (Zhang et al.) based on different normalization methods for TCS images.

Normalized dataset	$F(1,5,7)$	$F(61,77)$	$F(66,3)$	Confusion matrix
$\frac{X-\mu}{\sigma}$	67.39%	60.08%	70.29 %	$\left(\begin{smallmatrix} 66 & 1 \\ 40 & 31 \end{smallmatrix}\right)$
$[0, 255]$	65.94%	61.59 %	70.29%	$\left(\begin{smallmatrix} 60 & 7 \\ 34 & 37 \end{smallmatrix}\right)$
Exponential	63.76%	60.14%	78.26%	$\left(\begin{smallmatrix} 61 & 6 \\ 24 & 47 \end{smallmatrix}\right)$
Rayleigh	30.43%	68.84%	77.53%	$\left(\begin{smallmatrix} 60 & 7 \\ 24 & 47 \end{smallmatrix}\right)$

that the rotation-invariant Gabor filter is better than the conventional Gabor filter. In addition, the rotation-invariant Gabor filter helps the SVM to separate between PD patients and healthy controls. In particular, the entropy feature is more stable than the mean and the standard deviation features in the monotonic change of the gray scale. One of the factors that determine the accuracy of the results is the manual segmentation of HoM area by physician. In our future work, we plan to develop an automatic segmentation algorithm for localization of the HoM area.

References

1. Becker G, Seufert J, Bogdahn U, et al. Degeneration of substantia nigra in chronic Parkinson's diseasvisualized by transcranial color-coded real-time sonograph. Neurology. 1995;45:182–4.
2. Behnke S, Berg D, Becker G. Does ultrasound disclose a vulnerability factor for Parkinson's disease? J Neural. 2003;250 Suppl 1:I24–I2.
3. Hagenah JM, Hedrich K, Becker B, et al. Distinguishing early-onset PD from dopa-responsive dystonia with transcranial sonography. Neurology. 2006;66:1951–52.
4. Kier C, Seidel G, Bregemann N, et al. Transcranial sonography as early indicator for genetic Parkinson's disease. Proc IFMBE. 2009; p. 456–9.
5. Chen L, Seidel G, Mertins A. Multiple feature extraction for early Parkinson risk assessment based on transcranial sonography image. Proc Int Conf Image Proc. 2010.
6. Chen L, Hagenah J, Mertins A. Texture analysis using gabor filter based on transcranial sonography image. Proc BVM. 2011; p. 249–53.
7. Han J, Ma KK. Rotation-invariant and scale-invariant gabor features for texture image retrieval. Image Vis Comput. 2007;25:1474–81.
8. D Zhang MI A Wong, Lu G. Content-based image retrival using gabor texture features. IEEE Trans Trans Pattern Anal Mach Intell. 2000; p. 13–5.
9. Manjunath BS, Ma WY. Texture features for browsing and retrieval of image data. IEEE Trans Pattern Anal Mach Intell. 1996;18:837–42.
10. Cover TM, Thomas JA. Elements of information theory. USA: John Wiley; 2006.
11. Zuiderveld K. Contrast limited adaptive histogram equalization. In: Heckbert PS, editor. Graphics gems IV. San Diego, CA, USA: Academic Press Professional, Inc.; 1994. p. 474–85.
12. Lazebnik S, Schmid C, Ponce J. A sparse texture representation using local affine regions. IEEE Trans Pattern Anal Mach Intell. 2005;27:1265–78.